Measurements of Black Carbon Specific Absorption in the Mexico City Metropolitan Area during the MCMA 2003 Field Campaign

J. C. Barnard, E. I. Kassianov, T. P. Ackerman, S. Frey, K. Johnson, B. Zuberi, L. T. Molina, M. J. Molina, J. S. Gaffney, N. A. Marley

Atmos. Chem. Phys. Discuss., 5, 4083–4113, 2005
www.atmos-chem-phys.org/acpd/5/4083/
SRef-ID: 1680-7375/acpd/2005-5-4083
European Geosciences Union

Atmospheric Chemistry and Physics Discussions

Measurements of Black Carbon Specific Absorption in the Mexico City Metropolitan Area during the MCMA 2003 Field Campaign

J. C. Barnard[1], E. I. Kassianov[1], T. P. Ackerman[1], S. Frey[2], K. Johnson[2], B. Zuberi[2,*], L. T. Molina[2], M. J. Molina[2], J. S. Gaffney[3], and N. A. Marley[3]

[1]Pacific Northwest National Laboratory, Richland, Washington, USA
[2]Massachusetts Institute of Technology, Cambridge, Massachusetts, USA
[3]Argonne National Laboratory, Argonne, Illinois, USA
[*]now at: GEO_2 Technologies, Weston, Massachusetts, USA

Received: 1 April 2005 – Accepted: 17 May 2005 – Published: 23 June 2005

Correspondence to: J. C. Barnard (james.barnard@pnl.gov)

Abstract

During the Mexico City Metropolitan Area (MCMA) field campaign of 2003, measurements of the shortwave radiation field, lidar backscatter, and atmospheric concentrations of black carbon (BC) permitted the inference of the BC carbon specific absorption, α_λ, defined as the absorption cross section per unit mass (with units of m^2/g). This diverse set of measurements allowed us to determine α_λ in two ways. These methods – labeled I and II – are distinguished from one another in the manner that the columnar concentration of BC (with units of mg/m^2) is determined. This concentration is found by using either surface measurements of BC concentration and lidar estimates of aerosol mixing heights, or a more rigorous method that relies on the columnar aerosol size distribution. The averaged values of α_λ derived from these methods agree to about 20%, although we expect that the values obtained from method I are underestimated. These results, along with those of Schuster et al. (2005), suggest that in the MCMA, α_λ is in a range of 8 to 10 m^2/g at a wavelength of 550 nm. This range is somewhat lower than the commonly accepted value of 10 m^2/g for a wavelength of 550 nm, but is consistent with the calculations of Fuller et al. (1999), who suggest that this value is too high.

1. Introduction

Black carbon is found throughout the atmosphere, is mostly of anthropogenic origin, and is thought to be the most important contributor to aerosol absorption of solar radiation. A key measure of the absorption efficiency of BC is the specific absorption, α_λ, defined as the absorption cross section per unit mass, typically given in units of m^2/g. The specific absorption is a function of wavelength, as indicated by the subscript λ. Over the years, the literature has reported a large range for values of α_λ, from as low as 2 m^2/g to as high as 25 m^2/g (e.g., Waggoner et al., 1981; Horvath, 1993; Liousse et al., 1993; Petzold et al., 1997; Penner et al., 1998; Moosmüller, 1998; Marley et al., 2001; Arnott et al., 2003; Schuster et al., 2005). As suggested by Liousse et al. (1993)

ACPD

5, 4083–4113, 2005

this wide variation may be caused by differences in the aerosol mixing state, with the smaller values favoring external mixtures, while larger values indicate internal mixing of BC. Estimates of aerosol radiative forcing attributable to BC are dramatically influenced by the mixing state of BC, and because of the relationship between mixing state and α_λ, these estimates depend on the value of α_λ as well (e.g., Riemer et al., 2003; Sato et al., 2003; Lesins et al., 2002; Chung and Seinfeld, 2002; Jacobson, 2001; Jacobson, 2000; Fuller et al., 1999; Chylek et al., 1995; Ackerman and Toon, 1981).

Because of the importance of α_λ in determining the magnitude of aerosol radiative forcing, atmospheric measurements of this quantity are of critical importance. In this paper, we present such measurements made within the Mexico City basin during the MCMA field campaign undertaken in April and May of 2003. This basin is an ideal place to study BC aerosols because of the high BC emissions; the high altitude, which enhances the aerosol scattering signal over that of molecular scattering; significant variations in relative humidity, from very dry to saturated conditions; and the unique meteorology of the Mexico City basin, which tends to flush out the pollutants on a daily basis (Molina et al., 2002; Whiteman et al., 2000; Fast and Zhong, 1998).

2. Methodology

2.1. Measurements

The MCMA field campaign deployed numerous instruments that permitted α_λ to be determined in two independent ways. The instruments used for the analysis presented here are listed in Table 1, which shows the quantities that are directly measured by the instruments as well as those that are inferred from these measurements. The instruments were deployed at the National Center for Environmental Research and Training (Centro Nacional de Investigación y Capacitatión Ambeintal, abbreviated as CENICA), on the Iztapalapa campus of the Unversidad Autónoma Metropolitana (UAM). This site is located at a latitude and longitude of 19.36 N and 99.07 W, respectively, and is atop

ACPD
5, 4083–4113, 2005

a building and is removed from direct exposure to automobile exhaust. Therefore, we expect that the BC aerosols observed here will be aged compared to those freshly emitted in traffic.

The Multi-Filter Rotating Shadowband Radiometer (MFRSR, Harrison et al., 1994) is, as the name implies, a shadowband radiometer that measures two components (diffuse and total) of the shortwave radiation field at the wavelengths specified in Table 1. The third component of the field – the direct component – is found from the total and diffuse components by subtraction combined with a correction for the cosine response of the instrument. Because all three radiation components are measured with the same sensor, if one component can be calibrated accurately, the other two components will share similar calibration accuracies. Typically, the direct component of the irradiance is calibrated in the field using the Langley method with a calibration accuracy that approaches 1% (Michalsky et al., 2001).

Aerosol optical thicknesses, τ_λ, are easily derived from the direct component, provided that the path between the sun and the instrument is not obscured by clouds. Whether this criterion is met is easily determined using the Ångström exponent, å (Seinfeld and Pandis, 1998). The single scattering albedo, $\varpi_{0,\lambda}$, is the probability ($0 \leq \varpi_{0,\lambda} \leq 1$) that an aerosol scatters, rather than absorbs, a photon that impinges on it. Formally it is the ratio of the aerosol scattering coefficient, b_{scat} (m^{-1}), to the aerosol extinction coefficient, which is the sum of the b_{scat} and absorption coefficient, b_{abs} (m^{-1}), or $\varpi_{0,\lambda} = b_{scat}/(b_{scat}+b_{abs})$. The single scattering albedo can be retrieved from the diffuse and total irradiances using the algorithm of Petters et al. (2003), Kassianov et al. (2005), or Goering et al. (2005). These algorithms work best for large optical thicknesses (e.g., $\tau_\lambda > 0.25$ at 500 nm), a condition that is frequently met in the Mexico City basin. For the work reported here, we tested both the Petters and Kassianov algorithms and obtained nearly similar results for retrieved single scattering albedos, suggesting that the results presented below are independent of the algorithm chosen. These algorithms can only be used if the sky is completely free of clouds, a criterion that was verified using the method of Long and Ackerman (2000).

ACPD
5, 4083–4113, 2005

The aethalometer (Hansen et al., 1984) measures BC concentrations using an optical method that relies on the light attenuation (at seven discrete wavelengths) across a filter exposed to ambient aerosols. The attenuation is assumed to be linearly related to the concentration of BC through a calibration coefficient that has been empirically determined by the manufacturer from comparison of the aethalometer optical data to thermal decomposition chemical data in multi-site studies. The accuracy of this coefficient is a subject of investigations (Weingartner et al., 2003; Saathoff et al., 2003; Sheridan et al., 2005; Arnott et al., 2005). These studies indicate that the calibration coefficient can vary with filter loading, and to reduce this impact, we operated the instrument in a "dilution mode". In this mode, the maximum filter loading is reduced by switching to a new filter when the attenuation through the filter reaches 10%, instead of the usual 25%. The standard calibration coefficient supplied by the manufacturer was used. Unlike other absorbing aerosol species (e.g., humic-like substances), the imaginary part of the refractive index for black carbon is relatively constant from the ultraviolet to the infrared (Marley et al., 2001). Thus, a comparison of results from the different wavelength channels can act as an independent validation of the assumption that BC is the main absorbing species in the samples. For the sampling period, all of the seven channels were found to be in excellent agreement, with a variation from 1–2%, indicating that black carbon was indeed the major light absorbing material present in the aerosol, if not the only one.

It would have been desirable to have made measurements of BC concentration using instruments that do not rely on optical methods (i.e., see Saathoff et al., 2003). Unfortunately, such measurements were not made. Had they been available, they would have had the potential to significantly bolster our confidence in the aethalometer measurements.

Figure 1 shows BC concentrations measured by the aethalometer, C_{BC}, during a two-day period of the MCMA field campaign beginning on 15 April 2003. For the two days depicted in this figure, a pronounced diurnal variation is evident that is typical of the BC concentration during the entire field campaign. This variation is caused by

ACPD
5, 4083–4113, 2005

several factors, including the emission rate of BC and the mixing of the BC upwards by the development of a convective boundary layer during the day. This last factor is particularly important. During late evening and in the early morning hours, the nocturnal boundary layer is stably stratified, thus trapping the BC close to the surface. As the sun heats the surface, a convective boundary layer forms that mixes the surface BC upwards throughout the atmosphere. This mixing commences prior to noontime and is noted in Fig. 1 by the pronounced drop in the surface BC concentrations.

The lidar used for this field study was a custom unit built at the Freie Universität Berlin (Frey et al., 2004). For this study, the main purpose of the lidar measurements is to provide an estimate of the vertical distribution of the aerosol. Three elastic backscatter measurements are made at wavelengths of 266 nm, 532 nm, and 1064 nm, as well as two Raman-shifted measurements. From the Raman measurements one can infer the vertical profile of aerosol extinction, but because of signal-to-noise issues, these retrievals are only practical for the nighttime hours. Fortunately, the vertical extent of the aerosol can still be estimated from the elastic backscatter. From these measurements, one can determine the aerosol mixing height as a function of time, $D(t)$, defined as the depth of the mixed layer below which we expect to find the bulk of the aerosols. Figure 2a shows these heights for two days beginning on 26 April 2003. Mixing heights, derived from the days during the field campaign when it was possible to infer a mixing height, are shown in Fig. 2b. This figure shows that the heights exhibit a diurnal variation reminiscent of the BC concentrations, and this variation is a direct manifestation of the development of a convective boundary layer during the day. As indicated in the figure, the aerosol mixing height can be quite deep during middle of the day (~4500 m), but it collapses quickly during the late afternoon hours as the emissions of the day are flushed from the basin. The figure also shows that the mixing heights are remarkably constant from day-to-day. We note parenthetically that the aerosol mixing heights obtained from the lidar are about 10% to 20% higher than the top of the boundary layer, as determined by potential temperature profiles. This implies that the aerosols are entrained above the top of boundary layer, the existence of a residual aerosol layer aloft,

ACPD
5, 4083–4113, 2005

or both.

Because the pollutants tend to be transported out of the basin on a daily basis, the pollution burden should mirror the amount of emissions on a given day. This conjecture is supported by the correlation between the columnar $\varpi_{0,\lambda}$ (500 nm) inferred from MFRSR measurements and estimates of the columnar concentration of BC, M_{BC}, obtained from aethalometer measurements of surface BC concentration and aerosol mixing heights. It is important to distinguish between the concentration of BC, C_{BC}, defined as the mass of BC per unit volume of air, and the "columnar concentration", M_{BC}, which is the mass of BC in an atmospheric column of unit area. To keep these two definitions distinct, the word "concentration" will refer to C_{BC}, while the words "columnar concentration" will refer to M_{BC}. (The method of finding M_{BC} is discussed below.) This correlation is shown in Fig. 3, in which M_{BC} is expressed in units of mg/m^2. The single scattering albedos represent a spatial average over the atmospheric column above the MFRSR, while both M_{BC} and $\varpi_{0,\lambda}$ are averaged over the time period that it was possible to infer $\varpi_{0,\lambda}$. It is unlikely that the strong correlation exhibited in Fig. 3 would be observed if pollutants lingered in the Mexico City (MC) basin for periods significantly longer than a day, because emissions from one day would be mixed with previous days' emissions (altered, of course, by chemical conversion, deposition, and other processes) resulting in a "smoothing" of the aerosol burden and $\varpi_{0,\lambda}$, with time. This argument is made *a fortiori* when considering the religious holiday (Holy Friday, 18 April 2003), when traffic and the corresponding emissions were significantly reduced. In Fig. 3, this day is represented by cross (+) and $\varpi_{0,\lambda}$ is high, indicating reduced aerosol absorption that is consistent with the reduced BC surface emissions for this particular day.

It is interesting to note that for Holy Friday, the amount of aerosol was significantly reduced compared to other days in the campaign. This reduction is evinced by the measurements of τ_λ listed in Table 2, which reveals that τ_λ is the lowest for this day when compared to the other days considered. Because $\varpi_{0,\lambda}$ is independent of the amount of aerosol – a so-called aerosol intensive property (Ogren, 1995) – the BC

ACPD
5, 4083–4113, 2005

fraction in the aerosol mix must be lower on Holy Friday than for other days. This supposition is confirmed below.

2.2. Determination of α_λ

The measurements described above form the basis of two methods for determining α_λ. These methods rely on the simple equation:

$$\alpha_\lambda = \frac{(1-\varpi_{0,\lambda})\tau_\lambda}{M_{BC}} = \frac{\tau_{\lambda,abs}}{M_{BC}}, \quad (1)$$

where $\tau_{\lambda,abs}$ is the aerosol absorption optical depth. The major assumption underlying this equation is that BC is the only atmospheric absorber at the wavelength λ, which is generally valid outside the UV and near-UV spectral ranges (Heintzenberg et al., 1997). The aerosol optical thickness is inferred from the MFRSR direct normal irradiances, and $\varpi_{0,\lambda}$ is found from the diffuse and total MFRSR irradiances and the single scattering albedo algorithms mentioned above. It then remains to find M_{BC}.

This quantity can be inferred in two ways, which define our method I and method II. These methods differ significantly in the assumptions that underlie them. The most approximate method, method I, makes use of the aerosol mixing heights mentioned above and the surface aethalometer concentrations. M_{BC} is found as the average of the product of $C_{BC}(t)D(t)$ over the time period when the skies were clear, and it was therefore possible to find $\varpi_{0,\lambda}$ and therefore α_λ. Formally,

$$M_{BC} = \int_{t_{begin}}^{t_{end}} C_{BC}(t)D(t)dt/(t_{begin}-t_{end}), \quad (2)$$

where t_{begin} and t_{end} bracket the time interval in question. These time intervals are listed in the first column of Table 2. Equation (2) is based on the assumption that the observed BC concentrations are well-mixed in the boundary layer below the mixing

height, and BC does not exist above the mixing height, and that C_{BC} obtained from the aethalometer is a reasonable measure of the columnar BC concentrations. The use of a surface measurement of BC as a proxy for the concentration throughout this mixed layer is supported by the strong correlation between surface BC measurements and $\varpi_{0,\lambda}$ (e.g., Fig. 3). That is, when the surface concentration is large, we expect that the columnar concentration will be large, and visa versa. Nevertheless, the assumption that underpins Eq. (2) – that the surface measurement C_{BC} is constant throughout the mixed layer – may not be closely satisfied, thus underscoring the approximate nature of this method. On the other hand, this method requires no assumptions about the BC physical parameters such as density and refractive indices, nor does it require any assumption about the mixing state of BC.

A completely different set of assumptions is required for method II. For this method, we assume that: (1) the aerosol is internally mixed in a shell/core manner (Jacobson, 2000), with the core of the aerosol consisting of BC, (2) the physical characteristics (density, ρ_{BC}; refractive index, $\tilde{m}_{BC}$) of the BC are known, (3) the shell is non-absorbing, and (4) the columnar aerosol volume distribution of the aerosol is known. The first assumption of an internal mixture is difficult to verify although electron micrographs of the aerosol, as well as a single-particle chemical analysis of the aerosols, indicate that the soot is internally mixed with other substances (Johnson et al., submitted, 2005[1]). Given the complexity of aerosol shapes and mixing configurations depicted in Johnson et al., the shell/core model of internal mixing is a simplification but is necessary for conventional Mie theory calculations of the aerosol's optical properties. In regards to the second assumption, the reported values for the physical properties of BC vary widely as reported by Fuller et al. (1999). Lacking in situ measurements we assume plausible values for these properties, listed below. The third assumption is supported by the aethalometer measurements that suggest that BC is the only ab-

[1]Johnson, K. S., Zuberi, B., Molina, L. T., Molina, M. J., Laskin, A., and Cowin, J. P.: Processing of soot in an urban environment: case study from the Mexico City Metropolitan Area, submitted to Atmos. Chem. Phys., 2005.

ACPD
5, 4083–4113, 2005

sorber in the wavelength region considered here. Thus it is reasonable to assume that the shell does not absorb.

The columnar aerosol volume distribution, required by the fourth assumption, is obtained from Dubovik et al. (2002). They used data from a sun photometer located in Mexico City, part of the AERONET (Aerosol Robotic Network) project (Holben et al., 1998), to find volume distributions and other aerosol parameters. The volume distribution found by the AERONET algorithm is expressed as $dV/dlnr$ with units ($\mu m^3/\mu m^2$), such that the integration over all aerosol radii (or more properly, the logarithm of the aerosol radius) yields the total volume concentration of the aerosol per unit area of the atmospheric column, C_V (with units $\mu m^3/\mu m^2$). The inversion method leading to the aerosol volume distribution, as well as the assumptions inherent to the inversion (e.g., spherical particles, various smoothing constraints), have been discussed in Dubovik and King (2000). Formally, the volume distribution is the sum of two lognormal distributions that represent the fine (f) and coarse modes (c) of the total distribution,

$$\frac{dV(r)}{d\ln r} = \frac{C_{V,f}}{\sqrt{2\pi}\sigma_f}\exp\left[-\frac{(\ln r - \ln r_{V,f})^2}{2\sigma_f^2}\right] + \frac{C_{V,c}}{\sqrt{2\pi}\sigma_c}\exp\left[-\frac{(\ln r - \ln r_{V,c})^2}{2\sigma_c^2}\right]. \quad (3)$$

In this equation, r the is particle radius, r_V and σ are the median particle radius and the standard deviation, respectively, for either the fine or coarse mode. For the MCMA, the coefficients needed for Eq. (3) are listed in Table 1 of Dubovik et al. (2002), and for the sake of convenience we list them here. The fine mode parameters are: $C_{V,f}$=0.12$\tau_{\lambda=440\,nm}$±0.03 ($\mu m^3/\mu m^2$), $r_{V,f}$=0.12+0.04$\tau_{\lambda=440nm}$±0.04 (μm), σ_f=0.43±0.03, while the coarse mode parameters are: $C_{V,c}$=0.11$\tau_{\lambda=440\,nm}$±0.03 ($\mu m^3/\mu m^2$), $r_{V,c}$=2.72+0.60$\tau_{\lambda=440\,nm}$±0.23 (μm), σ_c= 0.63±0.05. The optical thickness at 440 nm can be determined from the MFRSR optical thickness inferred at 500 nm using the Ångström relationship.

ACPD
5, 4083–4113, 2005

Finding M_{BC} using the method II is more complicated than method I. We begin with the equations

$$(1 - \varpi_{0,\lambda})\tau_\lambda = \int_0^\infty \frac{dn(r)}{dr}\sigma_{abs}(\tilde{m}_s, \tilde{m}_{BC}, r, f_V)dr \quad (4)$$

and

$$\tau_\lambda = \int_0^\infty \frac{dn(r)}{dr}\sigma_{ext}(\tilde{m}_s, \tilde{m}_{BC}, r, f_V)dr\,, \quad (5)$$

where $dn(r)/dr$ is columnar number distribution obtained from the volume distribution (e.g., $dV/dlnr{=}r(4/3\pi r^3)dn(r)/dr$); $\sigma_{abs}(\tilde{m}_s, \tilde{m}_{BC}, r, f_V)$ and $\sigma_{ext}(\tilde{m}_s, \tilde{m}_{BC}, r, f_V)$are the absorption and extinction cross sections as a function of the (complex) refractive indices of the shell, $\tilde{m}_s$, and the BC core, $\tilde{m}_{BC}$; r is the total radius of the particle, and f_V ($0 \leq f_V \leq 1$) is the volume fraction of the aerosol that consists of BC. Invoking assumptions two and three mentioned above, we assume values for $\tilde{m}_{BC}$ and the complex part of $\tilde{m}_s$, denoted as Im[$\tilde{m}_s$]; $dn(r)/dr$ is known from the AERONET retrievals, and from the MFRSR measurements we can infer τ_λ and $\varpi_{0,\lambda}$. With these known factors, Eqs. (4) and (5) become integral equations for f_V and the real part of $\tilde{m}_s$, Re[$\tilde{m}_s$]. Once f_V is known, M_{BC} follows immediately,$M_{BC}{=}C_V f_V \rho_{BC}$, where again, we use assumption (2) and choose a plausible value for ρ_{BC}. We take ρ_{BC} equal to 2.0 g/cm^3 (Fuller et al., 1999) so that our results can be easily compared with those of Schuster et al. (2005), as will be explained in Sect. 3.

Solving Eqs. (4) and (5) for f_V and the real part of $\tilde{m}_s$ is a straightforward, iterative process. First, we assume values for $\tilde{m}_{BC}$ and Im[$\tilde{m}_s$], these are 2.0–1.0i (Fuller et al., 1999) and $-10^{-7}i$, respectively. The small imaginary part of the shell refractive index implies negligible absorption and is representative of a sulfate-like compound (Toon et al., 1976). Next, the shell/core Mie code of Ackerman and Toon (1981) is used to compute $\sigma_{abs}(\tilde{m}_s, \tilde{m}_{BC}, r, f_V)$ and $\sigma_{ext}(\tilde{m}_s, \tilde{m}_{BC}, r, f_V)$ for ranges of r that encompass

the limits of *dn(r)/dr* and plausible values of f_V. Equations (4) and (5) are integrated numerically, compared with $(1–\varpi_{0,\lambda})\tau_\lambda$ and τ_λ, respectively, and this process is repeated until the left- and right-hand sides of the equations are equal. This iteration is robust and converges rapidly.

When solving Eqs. (4) and (5), explicit knowledge of the columnar mass of BC is not necessary. We do not solve for the mass directly but instead find f_V. The mass enters into the specific absorption formula, $(1–\varpi_{0,\lambda})\tau_\lambda/(C_V f_V \rho_{BC})$ through the specification of ρ_{BC}. Recent measurements of the density of diesel soot (Park et al., 2004), and the discussion provided in Fuller et al. (1999) and Schuster et al. (2005) suggest a plausible range of ρ_{BC} from 1.7 to 2.0 g/cm^3. If the actual density in the MCMA is closer to 1.7 g/cm^3 than our assumed 2.0 g/cm^3, then the α_λ values reported here will be about 18% too low. Additionally, Schuster et al. (2005), using a technique similar to that described above, have estimated the error in M_{BC} retrievals to range from –40% to +15%. A large part of the uncertainty stems for the assumption of a water host encapsulating the BC and an ammonium sulfate inclusion, when in fact, water may not be present in the aerosol. As mentioned below in Sect. 3.3, the MCMA boundary layer was very dry when our observations were made, and correspondingly, the aerosols were likely dry. The existence of these dry aerosols considerably reduces the uncertainty of Schuster et al.'s original estimate, and accounting for the dryness reduces the uncertainty range in M_{BC} retrievals to –25% to +15%, including the uncertainty in ρ_{BC}.

3. Results

3.1. Specific absorption values

The techniques described above were applied to 7 cases during which the sky was free from clouds. These cases are listed in Table 2 along with the results from methods I and II for a wavelength of 500 nm. It is again important to reiterate that the derived values of α_λ are only appropriate for the time periods when the skies are clear because this

requirement is necessary to derive $\varpi_{0,\lambda}$. These time periods are indicated in Table 2 and occur in the morning hours, before a convective boundary layer develops that encourages the development of convective cloudiness. Table 2 show values of τ_λ , å, and $\varpi_{0,\lambda}$ averaged over the indicated clear sky periods.

The last three columns show α_λ for the seven cases considered here, derived from either method I or method II, and Re[$\tilde{m}_s$]. The specific absorptions are depicted by the bar chart in Fig. 4, which show that on a case-by-case basis, the two methods do not track each other. When averaged over the 7 cases, the averaged values, shown in the bottom row of Table 2, are 7.5 and 9.2, for methods I and II respectively – a difference of about 20%. It is also interesting to note that the values obtained from method II are relatively constant, in contrast to method I, in which significant fluctuations are seen from day-to-day. Over all days, the derived values of Re[$\tilde{m}_s$] are remarkably constant and are close to commonly quoted value for ammonium sulfate, 1.53 (Toon et al., 1976). This finding is consistent with a chemical analysis of single aerosol particles made during the MCMA campaign that reveals the sulfate composition of the aerosol increases as the aerosol ages[1].

Schuster et al. (2005) report values of α_λ at many AERONET locations using retrievals of aerosol properties from the AERONET sun photometers. The methodology behind their results closely parallels our method II. These two methods assume the same values for the physical properties of BC and the aerosol volume distribution. The major difference between the two methods is our use of a shell/core model to find aerosol optical properties versus the use of the Maxwell-Garnett (MG) effective medium approximation (Lesins et al., 2002; Bohren and Huffman, 1983) to find an "effective" refractive index of the aerosol mix. When using the MG approximation, the volume fractions of BC and ammonium sulphate, contained in a water host, are iterated until the difference between the calculated and observed (AERONET) values of the index of refraction is minimized. Once the volume fraction is known, M_{BC} is easily calculated.

For Mexico City, Schuster et al. (2005) quote a value of α_λ of 9.5±0.9 m^2/g when

averaged over the years 2000 and 2001, for a wavelength of 550 nm. Recall that our value 9.2 m^2/g has been derived for a wavelength of 500 nm, and to compare these two values, we must adjust our value to a wavelength of 550 nm. From measurements of α_λ taken at different wavelengths, Moosmüller et al. (1998) suggest that the wavelength dependence of α_λ is described by a power law, $\alpha_\lambda = C\lambda^{-2.7}$, where C is a constant. In contrast, Mie calculations using the AERONET volume distribution for Mexico City indicate a wavelength dependence of about λ^{-1}. Kirchstetter et al. (2004) suggest that the presence of organic carbon (OC) in an aerosol increases the dependence of aerosol absorption on wavelength, and that for motor vehicle aerosols that have a relatively large BC component, the wavelength dependence is about λ^{-1}, while for biomass smoke aerosols, with a relatively large organic carbon content, a wavelength dependence of approximately $\lambda^{-2}$is evident. Furthermore, as noted in Kirchsetter et al. (2004), OC most likely absorbs in the ultraviolet (UV) and near UV spectral regions. These considerations suggest that for our wavelength extrapolation, the relationship λ^{-1} is most appropriate. With this in mind, converting our "method II" value to 550 nm gives 8.4 m^2/g [=9.2 m^2/g(550nm/500 nm)$^{-1}$], and to the extent that this conversions is correct, the converted value is lower than Schuster et al.'s value by about 13%.

All values mentioned above are less than 10 m^2/g, a value commonly accepted for α_λ at a wavelength of 550 nm. These lower values are consistent with Fuller et al. (1999) who suggest that the "canonical" value is too large. They arrived at this conclusion by explicitly calculating α_λ for randomly spaced BC occlusions within a host sulphate aerosol, and these calculations indicate that α_λ>10 m^2/g occurs only when most of the BC is internally mixed, and the host aerosols are sufficiently large, defined as R_g>0.06 μm, where R_g is the conventional geometric mean radius. Our retrievals of R_g for the MCMA based on the algorithm of Kassianov et al. (2005), indicate that R_g is about 0.035 μm. Alternatively, using the fine component of the AERONET volume distribution yields an R_g of about 0.032 μm. Both of these radii are smaller that the 0.06 μm limit, suggesting that α_λ should be less than 10 m^2/g at 550 nm.

3.2. M_{BC}, f_v

In addition to α_λ, Table 2 provides other aerosol characteristics that are derived from our methods. Column seven lists M_{BC} as derived from methods I and II. All the M_{BC} values derived from method I are greater than or equal to the corresponding values from method II, and for methods I and II the average values of the seven cases are 4.7 and 3.7 mg/m^2, respectively. These are large BC loadings. As shown in Schuster (2004), columnar BC concentrations in an urban area (Goddard Space Flight Center [GSFC] near Washington, D.C., USA) inferred from AERONET measurements, can range as high as about 7 mg/m^2, although most values are less than 3 mg/m^2. That the BC columnar concentrations are larger than those at the GSFC seems intuitively plausible, given the very large population and emissions of the MCMA.

The fact that the method I columnar BC concentrations are larger than those derived from method II is a direct manifestation of the difference of assumptions that underlie the two methods. For method I, we assume that the BC concentration is constant throughout the mixed layer. In fact, however, the BC concentration is higher near the source – the surface – and decreases with height, in accordance with the gradient transport theories of turbulent transport. Thus, M_{BC} derived from method I is likely to be an overestimate of the actual M_{BC}, and correspondingly, α_λ, is likely to be an underestimate of the true α_λ. This tendency for underestimation is consistent with the results shown in Fig. 4, wherein it is evident that α_λ obtained from method I is generally less than α_λ obtained from method II.

Column six of Table 2 lists f_v – another variable that is derived as part of method II. The volume fraction is smallest for 18 April 2003 and is consistent with the high $\varpi_{0,\lambda}$ of that day.

3.3. Discussion

When the α_λ values derived from methods I and II are converted values appropriate for 550 nm using the conversion rule, λ^{-1}, and when averaged over all seven cases,

ACPD
5, 4083–4113, 2005

method I and II yield 6.8 m^2/g and 8.4 m^2/g, respectively. On the other hand, Schuster et al. (2005) derived a value of 9.5 m^2/g. These values span a plausible range as enunciated in Fuller at el. (1999), who state that for isolated carbon spheres, α_λ is about 5 m^2/g, while for aggregates of graphitic carbon grains, α_λ is about 7 m^2/g or less, and for occluded carbon, α_λ is unlikely to exceed 10 m^2/g, except for large, internally mixed aerosols. (Of course, the exact values of these boundaries depend on the size distribution of the aerosol, as well as the optical constants assumed for BC.) As previously mentioned, the evidence from Johnson et al. (submitted, 2005)[1] suggests that the aerosols are internally mixed, yet the aerosols over the MCMA are are probably not large enough to expect α_λ>10 m^2/g. Our low α_λ value (for method I) is consistent with an externally mixed aerosol, in which the BC consists of chains of carbon spherules and/or isolated carbon spherules, however, as mentioned above, we think the method I values are underestimates of the true magnitude of α_λ. Removing these values from consideration, our average value (8.4 m^2/g) and that of Schuster et al. (2005)(9.5 m^2/g) indicate that α_λ lies in a range of about 8–10 m^2/g at 550 nm.

It is reassuring that there is only a small discrepancy between these two values. However, because our method II uses the same BC physical/optical constants and the same volume distributions as Schuster et al., it is interesting to investigate why the observed difference exists. It cannot be completely explained by the different ways of dealing with the internal mixture, e.g., shell/core versus MG. For internal mixtures, Lesins et al. (2002) examined shell/core configurations and refractive index mixing rules such as MG. Optical properties derived from these two scenarios, for the same volume fraction of BC, were typically within 5% of one another. Using an aerosol volume distribution appropriate for the GSFC, Schuster et al.(2005) found that shell/core and MG approaches are similar, except for lower volume fractions of BC, f_V<0.2. For very small f_V (<0.05), the shell/core method gave higher specific absorptions than MG by at least 10%. These findings indicate that our results should be about 5–10% larger than Shuster et al.'s α_λ values. However, our shell/core values are smaller than Schuster et al.'s values.

Seeking other explanations for the discrepancy, we posit three alternative hypotheses. These are: (1) temporal and spatial sampling differences, (2) contamination of some of the measurements by unusually large gaseous absorption (e.g., NO_2) or aerosol absorption by OC, and (3) assumptions regarding the refractive index of the host. Examining the first of these, we note that our measurements cover only one month of one year, and occur only during the morning hours. By contrast, Schuster et al.'s measurements span two years and could include times other than the morning. The spatial sampling is also problematic because the distance between the MFRSR and the AERONET instruments is about 16 km, and the possibility that the instruments observe different types of aerosols, different aerosol size distributions, etc., cannot be dismissed. For example, Fig. 5 shows simultaneous observations of aerosol optical thickness at 500 nm, taken at the MFRSR and AERONET sites on 27 April 2003. In the morning hours, these optical thicknesses are similar, but diverge as the day progresses. This increasing discrepancy can be explained by the meteorology of the MCMA (Fast and Zhong, 1998): the winds that arise during the morning often blow the pollution towards the AERONET site, thus increasing the optical thickness at this site over that at the MFRSR site. Whether this increasing optical thickness is associated with a change in aerosol intensive properties (e.g., $\varpi_{0,\lambda}$) cannot be determined without additional measurements.

The next hypothesis assumes some aerosol absorption occurs, which mistakenly is attributed to BC, when it is in fact caused by other substances. This absorption, if not properly accounted for, would raise the value of α_λ. Two possible sources of "mistaken" absorption are OC or NO_2. For example, observations of surface NO_2 concentrations that occur in the morning hours in Mexico City (R. Volkamer, personal communication) show that it is large enough (>40 ppb) to be a significant absorber. These high concentrations would contaminate the retrievals of $\varpi_{0,\lambda}$ at wavelengths where there is significant NO_2 absorption (440 nm for the AERONET sun photometer and 415 nm for the MFRSR). The effect of this absorption is to reduce the inferred value of $\varpi_{0,\lambda}$ compared to the value that would be inferred if the NO_2 absorption were

properly taken into account. Because we were concerned about this problem, we did not attempt any α_λ retrievals for the 415-nm channel of the MFRSR. Without repeating the analysis of Schuster et al., we cannot determine to what extent NO_2 contamination influences their results or indeed whether NO_2 contamination was occurring.

Third, values for the real part of the host refractive index, either retrieved in our methodology, or obtained from the AERONET inversions in the case of Schuster at al., can significantly influence specific absorption retrievals. For example, if we assume that the real part of the host refractive index is known and equal to 1.33, appropriate for a water shell, and we find f_v from Eq. (4) only, the specific absorption values are increased by about 40%. This assumption, however, causes the computed τ_λ from Eq. (5) to be significantly less than those observed. We note that the real part of the refractive index for Mexico City quoted in Dubovik et al. (2002) is 1.47, somewhat less than our retrieved values of about 1.56. This difference would suggest that our derived α_λ values would be less than those of Schuster et al. (2005) because as $\mathrm{Re}[\tilde{m}_s]$ increases, α_λ decreases. A retrieval of a relatively large value of $\mathrm{Re}[\tilde{m}_s]$ is consistent with the dry boundary layer in the MCMA during the 2003 field campaign in the morning hours. For example, at 06:00 AM and noon, local standard time, soundings show that the relative humidity below the aerosol mixing height is 30% or less (except right at the surface), and it decreases as the morning progresses. At these low humidities the aerosol is probably dry leading to larger $\mathrm{Re}[\tilde{m}_s]$ and less absorption by BC (Redemann et al., 2001).

4. Conclusions

Using data from the MFRSR, an aethalometer, and a lidar, as well as aerosol volume distributions obtained from the AERONET sun photometer, we calculated α_λ during the MCMA-2003 field campaign, for a wavelength of 500 nm. The diverse set of instruments permitted the calculation of α_λ using two methods, which differ significantly in approach and the assumptions that underlie these approaches. Both methods use

ACPD
5, 4083–4113, 2005

inferences of the aerosol optical thickness, τ_λ, and aerosol single scattering albedo, $\varpi_{0,\lambda}$, obtained from the MFRSR to estimate the absorption optical thickness, $\tau_{\lambda,abs}$. Once this quantity is estimated, all that is needed is an estimate of columnar concentration of BC, M_{BC}. Using method I, M_{BC} is found from lidar estimates of the aerosol mixing height and surface BC concentrations from an aethalometer. Method II relies on the AERONET volume distribution, the assumption of a shell/core model of internal mixing, and specific choices of BC density and refractive index to find M_{BC}. When averaged over 7 clear periods of the MCMA-2003 field campaign, the values of α_λ are 7.5 m^2/g and 9.2 m^2/g, for methods I and II, respectively. This level of agreement seems reasonably good, given the marked differences between the two methods.

When converted to a wavelength of 550 nm using a λ^{-1} conversion rule, the values of α_λ are 6.8 m^2/g and 8.4 m^2/g, for methods I and II, respectively. For the aerosol size distributions observed in the MCMA, these values lie within the range of plausible α_λ values as demarcated by Fuller et al. (1999), although the lower value is somewhat too low to be in accordance with an internally mixed aerosol. However, the assumptions that underpin method I are not likely to be completely satisfied for reasons stated in Sect. 3.2 above, and we expect that α_λ values obtained from this method to be underestimated.

Schuster et al. (2005) have derived a α_λ value of 9.5 m^2/g at 550 nm, and this value is reasonably close to ours. Thus, given this information we conclude that α_λ has a value of between 8 and 10 m^2/g in the MCMA, for aerosols that are moderately aged, and for a BC density of 2.0 g/m^3.

Acknowledgements. The authors are grateful to the other participants in the MCMA-2003 field campaign for their useful discussions regarding this work. The authors also thank J. Hubbe for setting up the MFRSR in Mexico City and B. deFoy of MIT for providing us the relative humidity sounding data. We would also like to thank the AERONET program for the collection and analysis of sun photometer data, which led to the aerosol volume distributions used in this study. Discussions with G. Schuster are also greatly appreciated. This research was sponsored in part by the U.S. Department of Energy's Atmospheric Science Program (ASP) under Contract DE-AC06-76RLO 1830 at Pacific Northwest National Laboratory. The Pacific Northwest

National Laboratory is operated for the U.S. Department of Energy by the Battelle Memorial Institute. The MIT team would like to acknowledge financial support from the National Science Foundation (Award No. ATM-0308748) and the Mexico City Environmental Commission.

References

Ackerman, T. P. and Toon, O. B.: Absorption of visible radiation in atmosphere containing mixtures of absorbing and non-absorbing particles, Appl. Optics, 20, 3661–3668, 1981.

Arnott, W. P., Moosmüller, H., Sheridan, P. J., Ogren, J. A., Raspet, R., Slaton, W. V., Hand, J. L, Kreidenweis, S. M., and Collett, J. L.: Photoacoustic and filter-based ambient aerosol light absorption measurements: Instrument comparisons and the role of relative humidity, J. Geo. Res.-A, 108 (D1), 4034, doi:10.1029/2002JD002165, 2003.

Arnott, W. P., Hamasha, K., Moosmüller, H., Sheridan, P. J., and Ogren, J. A.: Towards aerosol light-absorption measurements with a 7-wavelength Aethalometer: Evaluation with a photoacoustic instrument and 3-wavelength nephelometer, Aeros. Sci. T., 39 (1), 17–29, 2005.

Borhen, C. F. and Huffman, D. R.: Absorption and scattering of light by small particles, John Wiley & Sons, New York, 1983.

Chung, S. H. and Seinfeld, J. H.: Global distribution and climate forcing of carbonaceous aerosols, J. Geo. Res.-A, 107 (D19), 4407, doi:10.1029/2001JD001397, 2002.

Chylek, P., Videen, G., Ngo, D., Pinnick, R. G., and Klett, J. D.: Effect of black carbon on the optical-properties and climate forcing of sulfate aerosols, J. Geo. Res.-A, 100 (D8), 16 325–16 332, 1995.

Dubovik, O. and King, M. D.: A flexible inversion algorithm for retrieval of aerosol optical properties from sun and sky radiance measurements, J. Geo. Res.-A, 105 (D16), 20 673–20 696, 2000.

Dubovik, O., Holben, B., Eck, T. F., Smirnov, A., Kaufman, Y. J., King, M. D., Tanré, D., and Slutsker, I.: Variability of absorption amd optical properties of key aerosol types observed in worldwide locations, J. Atmos. Sci., 59, 590–608, 2002.

Fast, J. D. and Zhong. S. Y.: Meteorological factors associated with inhomogeneous ozone concentrations within the Mexico City basin, J. Geo. Res.-A, 103 (D15), 18 927–18 946, 1998.

Frey, S., Molina, L. T., Molina, M. J., and Wöste, L.: Design and implementation of a com-

pact raman-lidar for ozone and aerosol measurements, European Space Agency, (Special Publication) ESA SP, 1 (561), 151–154, 2004.
Fuller, K. A., Malm, W. C., and Kreidenweis, S. M.: Effects of mixing on extinction by carbonaceous particles, J. Geo. Res.-A, 104 (D13), 15 941–15 954, 1999.
Goering, C. D., L'Ecuyer, T. S., Stephens, G. L., Slusser, J. R., Scott, G., Davis, J., Barnard, J. C., and Madronich, S.: Simultaneous retrievals of column ozone and aerosol optical properties from direct and diffuse solar irradiance measurements, J. Geo. Res.-A, 110, D05204, doi:10.1029/2004JD005330, 2005.
Hanson, A. D. A., Rosen, H., and Novakov, T.: The aethalometer – An instrument for the real-time measurement of optical absorption by aerosol particles, Sci. Tot. E., 36, 191–196, 1984.
Harrison, L., Michalsky, J., and Berndt, J.: Automated multifilter rotating shadow-band radiometer: an instrument for optical depth and radiation measurements, Appl. Optics, 33, 5118–5125, 1994.
Heintzenberg, J., Charlson, R. J., Clarke, A. D., Liousse, C., Ramaswamy, V., Shine, K. P., Wendisch, M., and Helas, G.: Measurements and modeling of aerosol single-scattering albedo: Progress, problems, and prospects, Beitr. Phys. Atmosph., 70, 249–263, 1997.
Holben, B. N., Eck, T. F., Slutsker, I., Tanre, D., Buis, J. P., Setzer, A., Vermote, E., Reagan, J. A., Kaufman, Y., Nakajima, T., Lavenu, F., Jankowiak, I., and Smirnov, A.: AERONET – A federated instrument network and data archive for aerosol characterization, Remot. Sen. E., 66, 1–16, 1998.
Horvath, H.: Atmospheric light-absorption - a review, Atmos. Envir., 27 (3), 293–317, 1993.
Jacobson, M. Z.: A physically-based treatment of elemental carbon optics: Implications for global direct forcing of aerosols, Geophys. R. L., 27 (2), 217–220, 2000.
Jacobson, M. Z.: Strong radiative heating due to the mixing state of black carbon in atmospheric aerosols, Nature, 409 (6821), 695–697, 2001.
Kassianov, E. I., Barnard, J. C., and Ackerman, T. P.: Retrieval of aerosol microphysical properties using surface MFRSR data: Modeling and observations, J. Geo. Res.-A, 110, D09201, doi:10.1029/2004JD005337, 2005.
Kirchstetter, T. W., Novakov, T., and Hobbs, P. V.: Evidence that the spectral dependence of light absorption by aerosols is affected by organic carbon, J. Geo. Res.-A, 109, doi:10.1029/2004JD004999, 2004.
Lesins, G., Chylek, P., and Lohmann, U.: A study of internal and external mixing scenarios and

its effect on aerosol optical properties and direct radiative forcing, J. Geo. Res.-A, 107 (D10), 4094, doi:10.1029/2001JD00973,2002.
Liousse, C., Cachier, H., and Jennings, S. G.: Optical and thermal measurements of black carbon aerosol content in different environments - variation of the specific attenuation cross-section, sigma (sigma), Atmos. Envir., 27 (8), 1203–1211, 1993.
Long, C. N. and Ackerman, T. P.: Identification of clear skies from broadband pyranometer measurements and calculation of downwelling shortwave cloud effects, J. Geo. Res.-A, 105 (D12), 15 609–15 626, 2000.
Marley, N. A., Gaffney, J. S., Baird, C., Blazer, C. A., Drayton, P. J., and Frederick, J. E.: An empirical method for the determination of the complex refractive index of size-fractionated atmospheric aerosols for radiative transfer calculations, Aero. Sci. T., 34 (6), 535–549, 2001.
Michalsky, J. J., Schlemmer, J. A., Berkheiser, W. E., Berndt, J. L., Harrison, L. C., Laulainen, N. S., Larson, N. R., and Barnard, J. C.: Multi-year measurements of aerosol optical depth in the atmospheric radiation measurement and quantitative links programs., J. Geo. Res.-A, 106 (D11), 12 099–12 107, 2001.
Molina, M. J., Molina, L. T., West, J., Sosa, G., Sheinbaum-Pardo, C., San-Martini, F., Zavala, M. A., and McRae, G.: Air pollution science in the MCMA: Understanding source-receptor relationships through emissions inventories, measurements, and modeling, in: Air Quality in the Mexico Megacity: An Integrated Assessent, edited by: Molina, M. J. and Molina, L. T., Kluwer Academic Publishers, Dordrecht, The Netherlands, 137–202, 2002.
Moosmüller, H., Arnott, W. P., Rogers, C. F., Chow, J. C., Frazier, C. A., Sherman, L. E., and Dietrich, D. L.: Photoacoustic and filter measurements related to aerosol light absorption during the Northern Front Range Air Quality Study (Colorado 1996/1997), J. Geo. Res.-A, 103 (D21), 28 149–28 157, 1998.
Ogren, J. A.: In situ observations of aerosol optical properties, in: Aerosol Forcing of Climate, edited by: Charlson, R. J. and Heintzenberg, J., J. Wiley, Hoboken, New Jersey, USA, 215–226, 1995.
Park, K., Kittleson, D. B., Zachariah, M. R., and McMurry, P. H.: Measurement of inherent material density of nanoparticle agglomerates, J. Nanoparticle Res., 6, 267–272, 2004.
Penner, J. E., Chuang, C. C., and Grant, K.: Climate forcing by carbonaceous and sulfate aerosols, Clim. Dynam., 14 (12), 839–851, 1998.
Petters, J. L., Saxena, V. K., Slusser, J. R., Wenny, B. N., and Madronich, S.: Aerosol single scattering albedo retrieved from measurements of surface UV irradiance and a radiative

transfer model, J. Geo. Res.-A, 108 (D9), 4288, doi:10.1029/2002JD002360, 2003.
Petzold, A., Kopp, C., and Niessner, R.: The dependence of the specific attenuation cross-section on black carbon mass fraction and particle size, Atmos. Envir., 31 (5), 661–672, 1997.
Redemann, J., Russell, P. B., and Hamill, P.: Dependence of aerosol light absorption and single-scattering albedo on ambient relative humidity for sulfate aerosols with black carbon cores, J. Geo. Res.-A, 106 (D21), 27 485–27 495, 2001.
Riemer, N., Vogel, H., Vogel, B., and Fiedler, F.: Modeling aerosols on the mesoscale-gamma: Treatment of soot aerosol and its radiative effects, J. Geo. Res.-A, 108 (D19), 4601, doi:10.1029/2003JD003448, 2003.
Saathoff, H., Naumann, K.-H., Schnaiter, M., Schock, W., Weingartner, E., Baltensperger, U., Kramer, L., Bozoki, Z., Poschl, U., Niessner, R., Schurath, U.: Carbon mass determinations during the AIDA soot aerosol campaign 1999, J. Aerosol Sci., 34, 1399–1420, 2003.
Sato, M., Hansen, J., Koch, D., Lacis, A., Ruedy, R., Dubovik, O., Holben, B., Chin, M., and Novakov, T.: Global atmospheric black carbon inferred from AERONET, P. NAS US, 100, 6319–6324, 2003.
Schuster, G. L.: Inferring the specific absorption and concentration of black carbon from AERONET aerosol retrievals, Ph.D. thesis, The Pennsylvania State University, 2004.
Schuster, G. L., Dubovik, O., Holben, B. N., and Clothiaux, E. E.: Inferring black carbon content and specific absorption from AERONET retrievals, J. Geo. Res.-A, 101, D10S17, doi:10.1029/2004JD004548, 2005.
Seinfeld, J. H. and Pandis, S. N.: Atmospheric Chemistry and Physics, John Wiley & Sons, New York, 1998.
Sheridan, P. J., Arnott, W. P., Ogren, J. A., Andrews, E., Atkinson, D. B., Covert, D. S., Moosmüller, H., Petzold, A., Schmid, B., Strawa, A. W., Varma, R., and Virkkula, A.: The Reno Aerosol Optics Study: An evaluation of aerosol absorption measurement methods, Aeros. Sci. T., 39(1), 1–16, 2005.
Toon, O. B., Pollack, J. B., and Khare, B. N.: Optical constants of several atmospheric aerosol species – ammonium sulfate, aluminum oxide, and sodium chloride, J. Geo. Res., 81 (33), 5733–5748, 1976.
Waggoner, A. P., Weiss, R. E., Ahlquist, N. C., Covert, D. S., Will, S., and Charlson, R. J.: Optical characteristics of atmospheric aerosols, Atmos. Envir., 15 (10-1), 1891–1909, 1981.
Weingartner, E., Saathoff, H., Schnaiter, M., Streit, N., Bitnar, B., and Baltensperger, U.: Ab-

sorption of light by soot particles: determination of the absorption coefficient by means of aethalometers, J. Aeros. Sci., 34, 1445–1463, 2003.

Whiteman, C. D., Zhong, S., Bian, X., Fast, J. D., and Doran, J. C.: Boundary layer evolution and regional-scale diurnal circulations over the Mexico Basin and Mexican plateau, J. Geo. Res.-A, 105 (D8), 10 081–10 102, 2000.

Table 1. Instruments, the primary quantities measured by these instruments, and the quantities that can be inferred from the measurements.

Instrument	Primary Quantities measured	Inferred Quantities
MFRSR	Direct, diffuse, and total components of the solar radiation field at wavelenghths, λ=415, 500, 615, 673, 870, 940 nm	Aerosol optical thickness, τ_λ; single scattering albedo, $\varpi_{0,\lambda}$
aethalometer	Light attenuation	BC concentration in μg/m^3
lidar	Atmospheric backscatter at 532 nm	Aerosol mixing heights

Table 2. The 7 case studies selected for retrievals of α_λ (for λ=500 nm).

Date, time period (hours, LST)	τ_λ	å	$\varpi_{0,\lambda}$	$C_V=C_f+C_c$ ($\mu m^3/\mu m^2$)	f_V	M_{BC} (mg/m^2) I/II	α_λ (m^2/g) I	α_λ (m^2/g) II	Re[$\tilde{m}_s$]
14/4/2003 (08:26–10:19)	0.313	1.73	0.901	0.0898	0.01913	3.5/3.4	8.8	9.0	1.55
15/4/2003 (07:33–10:26)	0.331	1.50	0.889	0.0922	0.02230	5.3/4.1	7.0	8.9	1.57
16/4/2003 (08:02–10:27)	0.375	1.57	0.859	0.1054	0.02980	7.5/6.3	7.0	8.4	1.55
18/4/2003 (08:19–10:32)	0.267	1.48	0.965	0.0742	0.00577	0.86/0.86	10.8	10.9	1.59
26/4/2003 (07:36–10:40)	0.390	1.69	0.901	0.1113	0.01930	7.0/4.3	5.5	9.0	1.55
27/4/2003 (07:49–11:59)	0.310	1.69	0.924	0.0885	0.01401	3.6/2.3	6.6	9.5	1.56
30/4/2003 (07:54–11:00)	0.335	1.58	0.886	0.0943	0.02292	5.7/4.3	6.7	8.8	1.56
average						4.7/3.7	7.5	9.2	1.56

ACPD
5, 4083–4113, 2005

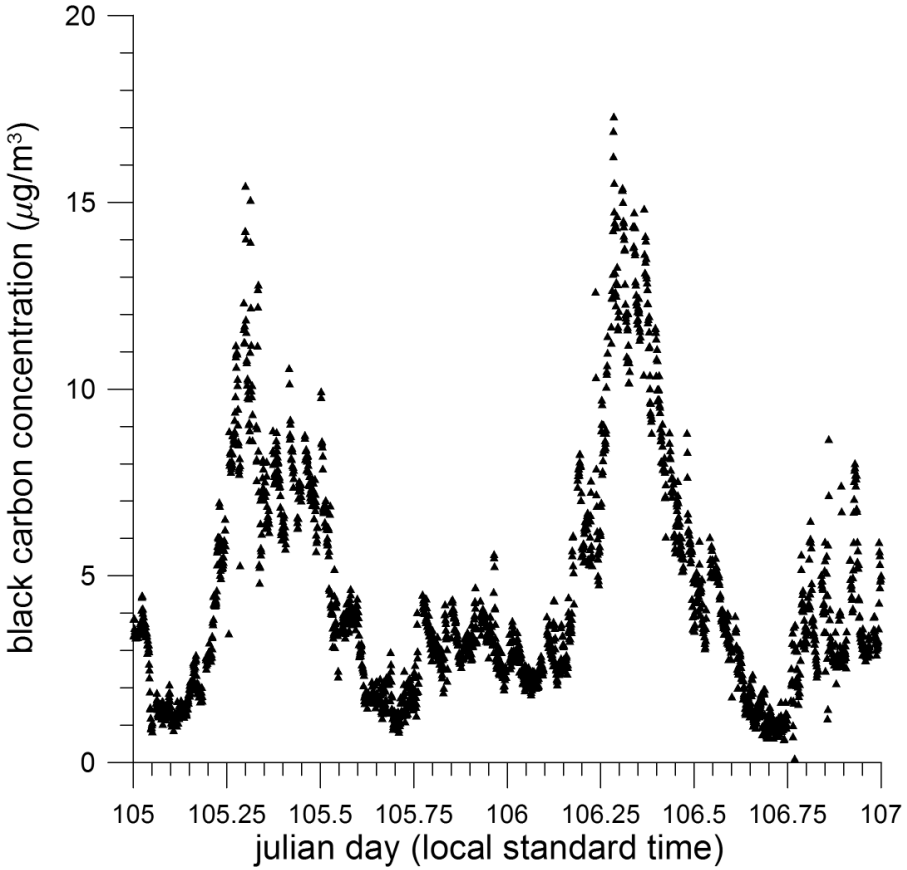

Fig. 1. Black carbon concentration (μg/m^3) as a function of time. Julian day 105 corresponds to 15 April 2003.

ACPD
5, 4083–4113, 2005

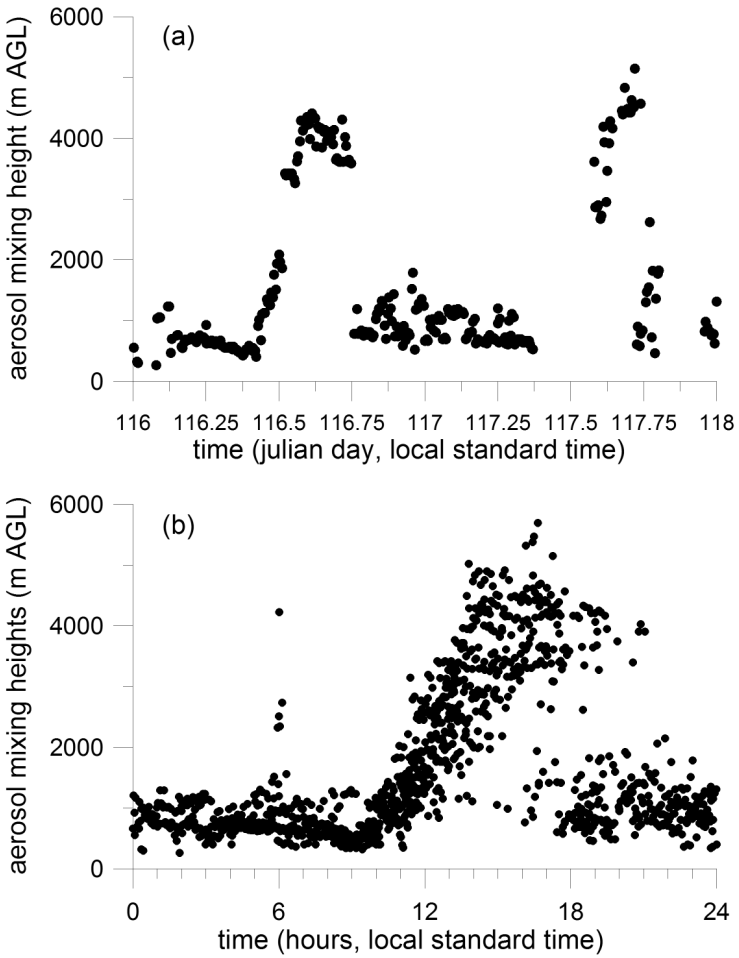

Fig. 2. Aerosol mixing heights as inferred from lidar backscatter data. Panel **(a)** shows at time series of the heights starting from julian day 116 (26 April 2003). Panel **(b)** shows all the mixing heights plotted versus time of day.

ACPD
5, 4083–4113, 2005

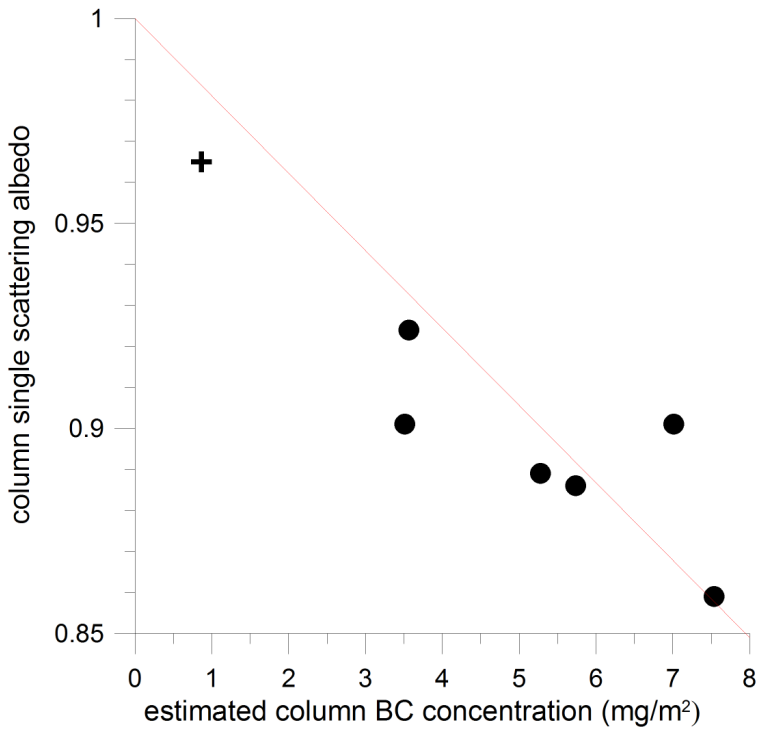

Fig. 3. Columnar single scatter albedo (500 nm) plotted versus the estimated columnar BC concentrations (with units mg/m^2). The symbol indicated by the cross (+) represents "Holy Friday" (18 April 2003), when emissions were significantly reduced because of the very light holiday traffic. The red line is a linear fit to these points, which is forced through the point (0 mg/m^2, $\varpi_{0,\lambda}$=1).

ACPD
5, 4083–4113, 2005

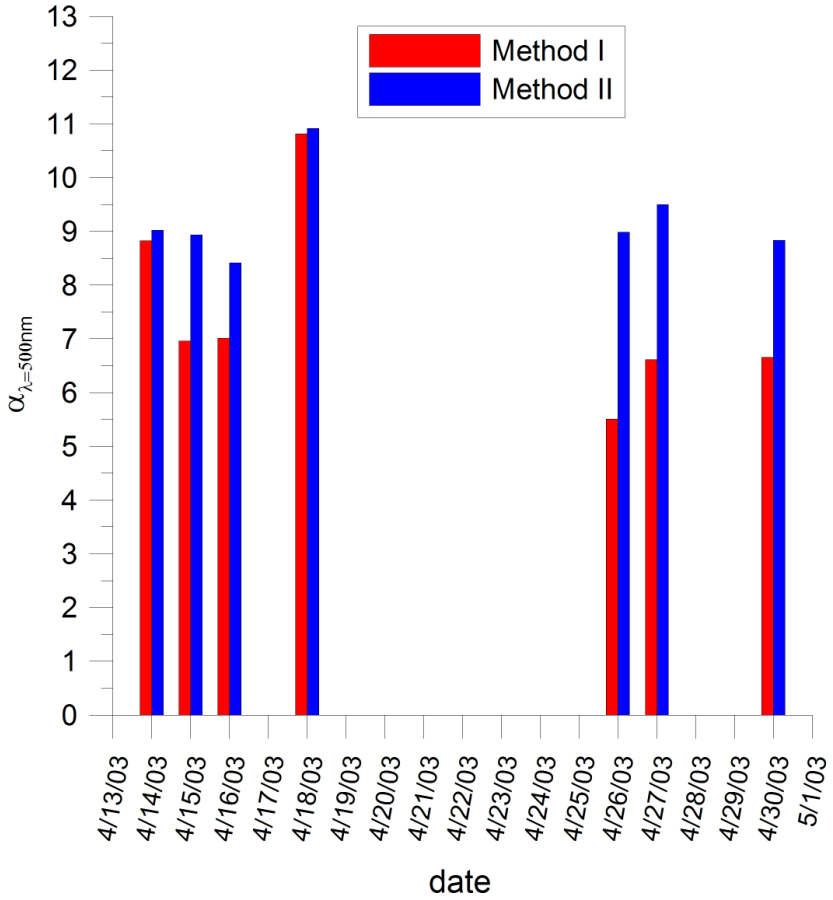

Fig. 4. Bar chart summarizing the values of α_λ, for λ=500 nm, over the course of the MCMA field campaign. Both methods I and II are shown.

ACPD
5, 4083–4113, 2005

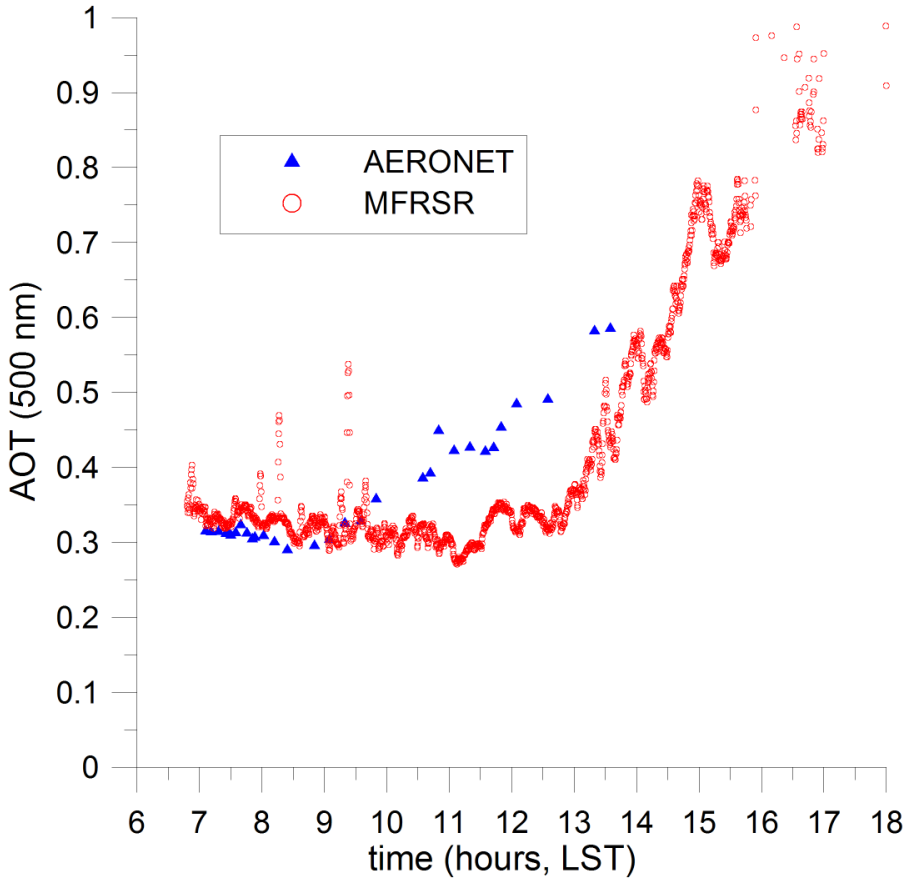

Fig. 5. Aerosol optical thickness (AOT) at 500 nm derived from the MFRSR and AERONET sun photometer in Mexico City. The date is 27 April 2003.

ACPD
5, 4083–4113, 2005